

Anomalous luminescence of Sm^{2+} in LaF_3 crystals

© E.A. Radzhabov

Vinogradov Institute of Geochemistry, Siberian Branch, Russian Academy of Sciences, Irkutsk, Russia

e-mail: eradzh@igc.irk.ru

Received January 17, 2025

Revised July 21, 2025

Accepted August 12, 2025

In $\text{LaF}_3\text{-Sm}^{2+}$ crystals, a broadband structureless luminescence band with a maximum at about 1230 nm was detected upon excitation into the region of $4f\text{-}5d$ transitions in samarium Sm^{2+} ions. By close analogy with the optical spectra of red luminescence in $\text{LaF}_3\text{-Eu}^{2+}$, the observed luminescence was attributed to anomalous luminescence.

Keywords: luminescence, lanthanides, samarium, absorption spectra

DOI: 10.61011/EOS.2025.08.62018.7541-25

Introduction

Besides the normal $5d\text{-}4f$ -luminescence, in most materials with Eu^{2+} and Yb^{2+} „anomalous“ broadband luminescence with a large Stokes shift is observed [1–3]. For such lanthanides, the excited $5d$ -level enters the conduction band. Luminescence occurs after transition from states of the conduction band, which have lower energy than the $5d$ -level, to the $4f$ -level of the lanthanide impurity ion [1,4,5]. The configuration coordinate scheme illustrating the origin of anomalous luminescence is detailed in previous studies [1,2].

Red $5d\text{-}4f$ -luminescence of divalent samarium in crystals has been actively studied recently due to interest in new scintillation [6–8,11–13] and dosimetric materials [9,10]. Samarium ions enter alkaline-earth fluoride crystals in the form of $2+$ or $3+$ ions. Both ions luminesce effectively. Emission Sm^{2+} is observed only at low temperatures, while Sm^{3+} luminesces also at room temperature. Divalent samarium luminesces in the red region in the range 650–900 nm [13]. Recent studies considered crystals $\text{CaF}_2\text{-Sm}^{2+}$, CsI-Eu,Sm^{2+} and CsI-Yb,Sm^{2+} as efficient red scintillators [14,15]. Crystals CsBr-Sm^{2+} , as expected, will be used in radio-photoluminescent dosimetry [16].

Broadband luminescence of Eu^{2+} in LaF_3 with a maximum at 600 nm also represents emission from relaxed states of the conduction band to the ground Eu $4f$ state (anomalous luminescence) [5].

In this work, broadband anomalous luminescence of Sm^{2+} was detected in LaF_3 crystals at low temperatures.

Experimental procedure

Crystals of LaF_3 , CeF_3 were grown by the Stockbarger method in a multibarrel graphite crucible in vacuum, creating a reducing atmosphere and leading to formation of divalent lanthanides in the crystals. Several percent

of CdF_2 was added to raw material to purify from oxygen impurities. The impurity concentration of SmF_3 in the blend was 0.01, 0.1, and 0.3 mol%. Crystals containing only Sm^{3+} were grown as well as crystals in which a significant fraction of trivalent samarium ions was converted to divalent form (hereafter designated as $\text{LaF}_3\text{-Sm}^{3+}$ and $\text{LaF}_3\text{-Sm}^{2+}$ respectively). The color of $\text{LaF}_3\text{-Sm}^{2+}$ crystals changed from light to dark green with increasing concentration of Sm^{2+} . Crystals $\text{LaF}_3\text{-Sm}^{3+}$, with only trivalent samarium were colorless. When divalent rare earths were added to LaF_3 crystals, charge-compensating anion vacancies formed in the lattice for electrical neutrality [17].

The content of Sm^{3+} was estimated by absorption lines, the most intense being the line at 399.5 nm and groups of lines around 1086, 1240, 1392 nm. In crystals $\text{LaF}_3\text{-0.01 mol% SmF}_3$ complete conversion of original Sm^{3+} into Sm^{2+} was observed. With increasing SmF_3 up to 0.1 and 0.3 mol%, the fraction of Sm^{2+} in grown crystals LaF_3 decreased.

Absorption spectra in the 190–3000 nm range were measured on a Perkin-Elmer Lambda-950 spectrophotometer, equipped with a low-temperature closed-cycle cryostat CCS-100/204N providing sample temperature 6.5–325 K. Emission spectra in the 200–890 nm range were measured through an MDR2 monochromator using a Hamamatsu H6780-04 photomodule. Emission spectra in the long-wavelength region were measured with a FEU83 photomultiplier tube (up to 1200 nm) and a cooled INGAAS photodiode IG17X3000Gli by Laser Components (up to 1700 nm). Semiconductor laser diodes at 405, 536, 650, 808, and 980 nm and a nitrogen laser LGI-21 (337 nm) were used for luminescence excitation.

The loss tangent ($\text{tg } \delta$) was controlled by an immittance meter E7–20 (MNIPI) in frequency range 25 Hz–1 MHz at temperatures 77–400 K.

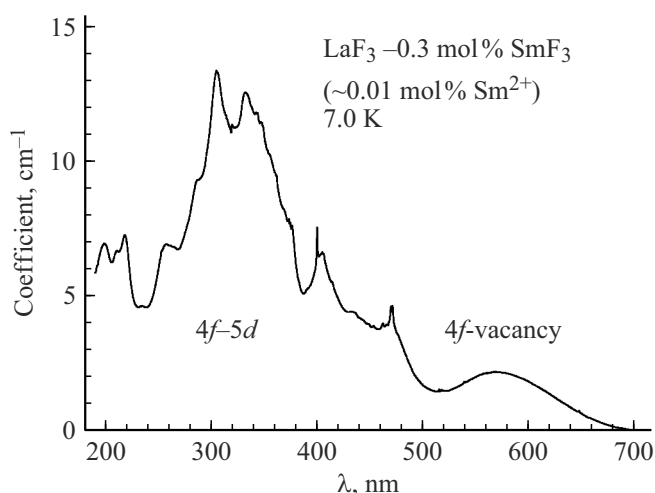


Figure 1. Absorption spectrum of $\text{LaF}_3\text{-}0.3 \text{ mol\% SmF}_3$ at 7.0 K. Estimated concentration of Sm^{2+} 0.01 mol%. Narrow absorption line near 400 nm belongs to Sm^{3+} ions; other bands belong to Sm^{2+} . The long-wavelength band corresponds to transitions from Sm^{2+} to a neighboring anion vacancy. The short-wavelength region below 500 nm is caused by $4f\text{-}5d$ -transitions in Sm^{2+} ion.

Results

Optical Spectra

In the absorption spectrum of $\text{LaF}_3\text{-Sm}^{2+}$ a broad structureless band with maximum near 600 nm and several bands at wavelengths shorter than 500 nm were observed (Fig. 1). Optical transitions of electrons from the $4f$ -shell of samarium ions to the $1s$ level of anion vacancy cause the long-wavelength absorption band with maximum near 580–600 nm, while transitions to $5d$ -shell levels cause short-wavelength absorption bands [5,12].

Excitation in the region of $4f\text{-}5d$ -transitions of Sm^{2+} showed a line emission spectrum 560–960 nm, caused by $4f\text{-}4f$ transitions in Sm^{2+} $^5D_{0,1,2}\text{-}^7F_j$ ions [12,16,18]. Additionally, at low temperatures a broad structureless luminescence band with a maximum near 1230 nm appears (Fig. 2).

The emission spectrum fits well with a Gaussian curve (Fig. 2). On the long-wavelength side, a small additional band with maximum near 1500 nm (6600 cm^{-1}) is observed (Fig. 2). The shape of the infrared band in crystals LaF_3 with 0.01, 0.1 and 0.3 mol% SmF_3 is identical.

The infrared band was observed under illumination by lasers at wavelengths 405, 450, 536 nm (region $4f\text{-}5d$ -transitions in Sm^{2+}). Radiation of longer wavelength lasers (650, 808, and 980 nm) did not excite the infrared band.

The intensity of $4f\text{-}4f$ -lines of Sm^{2+} continuously decreases above 7 K and is fully quenched near 180 K (Fig. 3). Conversely, the broadband emission at 1230 nm grows until about 130 K, then decreases, with luminescence quenched above 240 K (Fig. 3). The quenching of $4f\text{-}4f$ -emission in the 7–150 K range is caused by thermal escape of electrons

from the excited $4f$ -level to the conduction band, which may induce growth of anomalous luminescence as observed in Fig. 3.

The decay of infrared luminescence was measured under excitation by nitrogen laser LGI-21 at 337 nm. At 85 K, the decay of broadband emission in $\text{LaF}_3\text{-}0.1 \text{ Sm}^{2+}$ and $\text{LaF}_3\text{-}0.01 \text{ Sm}^{2+}$ in the 980–1070 nm range is described by two exponentials with lifetimes of 4.5 and $30 \mu\text{s}$ (Fig. 4). In $\text{LaF}_3\text{-Eu}$ crystals, lifetimes of anomalous luminescence were 2.2 and $13 \mu\text{s}$ at 7.6 K [5], close to these values $\text{LaF}_3\text{-Sm}^{2+}$.

In the excitation spectrum of broadband emission, bands were observed at 415 and 480 nm. In excitation spectra of $f\text{-}f$ luminescence of Sm^{2+} at 80 K, bands at 485, 415, and 330 nm were observed [12]. The excitation spectra of broadband infrared emission and line-like $4f\text{-}4f$ -emission Sm^{2+} in LaF_3 are close.

The absorption spectra and $4f\text{-}4f$ luminescence spectra caused by Sm^{2+} are similar in CeF_3 and LaF_3 crystals. Unlike $\text{LaF}_3\text{-Sm}^{2+}$ broadband luminescence in the wavelength range 600–1700 nm was not detected at cooling to 7 K in $\text{CeF}_3\text{-Sm}^{2+}$ crystals.

Dielectric losses

Due to the negative effective charge of the divalent ion in the LaF_3 lattice, an anion vacancy is located next to

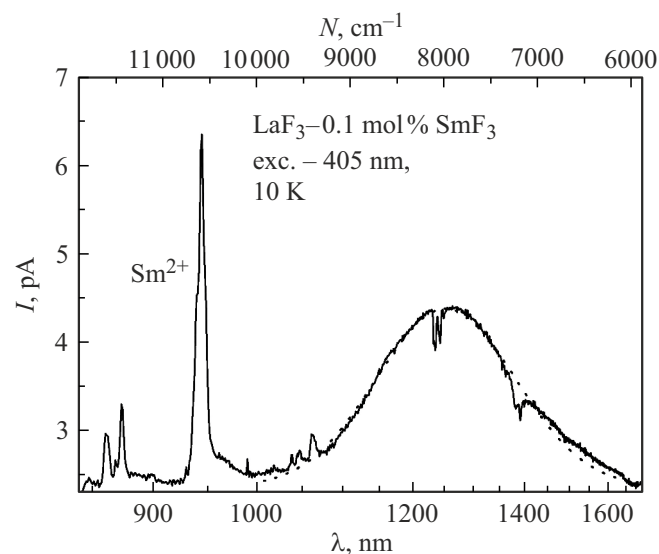


Figure 2. Emission spectrum of $\text{LaF}_3\text{-}0.1 \text{ mol\% SmF}_3$ at 10 K. The broad band around 1230 nm is well approximated by a Gaussian curve with parameters $N_{\text{max}} = 7980 \text{ cm}^{-1}$ and half-width $H = 1750 \text{ cm}^{-1}$ (dashed curve). For correct display of the Gaussian curve, the spectrum is displayed in energy units (cm^{-1} — upper scale), making the lower scale in nm nonlinear. Peaks at wavelengths shorter than 1100 nm are caused by $f\text{-}f$ -transitions in Sm^{2+} ions. Small dips near 1240 and 1380 nm are due to water vapor (hydroxyl) absorption in air. Lines near 870 and 940 nm are caused by transitions between 5D_0 - and 7F_5 , 7F_6 -levels in Sm^{2+} ions in LaF_3 respectively. The luminescence spectrum of $\text{LaF}_3\text{-Sm}^{2+}$ below 850 nm with interpretation was published earlier [21].

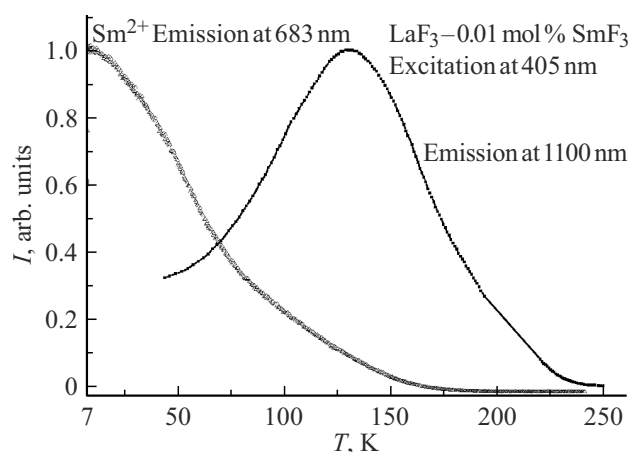


Figure 3. Temperature dependence of the emission intensity of the 683 nm line of Sm^{2+} and broadband luminescence at 1230 nm (measured at 1100 nm) in LaF_3 -0.01 mol% SmF_3 under 405 nm excitation. Similar curves were observed on heating and cooling, excluding thermally stimulated processes.

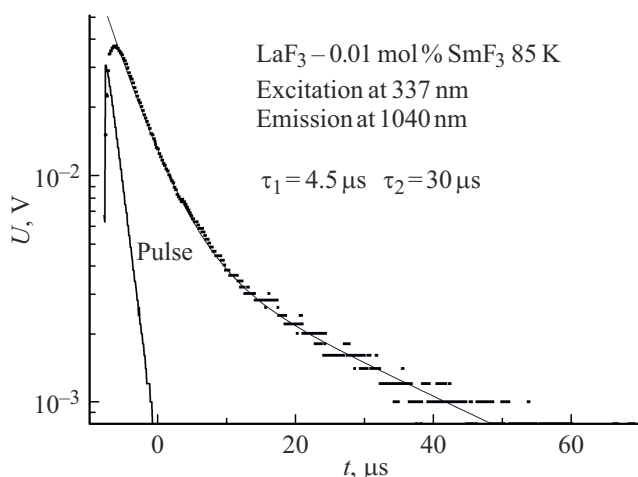


Figure 4. Decay of broadband emission at 1230 nm in LaF_3 -0.01 mol% SmF_3 upon excitation by nitrogen laser 337 nm at 85 K.

it, which leads to the appearance of a peak on the frequency dependence curve of the tangent of dielectric losses (Fig. 5). Similar loss tangent peaks were also observed in CeF_3 crystals doped with Sm^{2+} and other divalent ions. Measurement of the temperature dependence of the loss tangent allowed the estimation of the reorientation energy of the anion vacancy around divalent ions Sm^{2+} , Yb^{2+} , Eu^{2+} in LaF_3 [12,19,21 20].

Discussion

Similar structureless long-wavelength luminescence bands were observed in alkaline earth fluoride crystals under excitation of Eu^{2+} , Yb^{2+} in the $4f$ - $5d$ transition region and were called anomalous luminescence bands [1,4].

In the excitation spectrum of the broadband luminescence at 1230 nm, bands were observed at 410 and 480 nm. Broadband infrared luminescence at 1230 nm in LaF_3 - Sm^{2+} is excited by light from the $4f$ - $5d$ - transition region of Sm^{2+} (200–500 nm), whereas when excited by longer wavelength light from transitions from Sm^{2+} to anion vacancy (500–700 nm) (Fig. 1, $4f$ -vacancy) luminescence at 1230 nm is not excited. Since the excited $5d$ levels of Sm^{2+} in LaF_3 crystals enter the conduction band [21], it can be assumed that the observed broadband luminescence at 1230 nm corresponds to anomalous luminescence.

It is assumed that the excited $4f$ states can compete with the filling of band states, from which anomalous luminescence transitions may occur. Of the four energetically possible divalent lanthanides (Sm, Eu, Tm, Yb) for anomalous luminescence, luminescence was observed only for Eu and Yb. Anomalous luminescence for Sm^{2+} and Tm^{2+} is considered impossible (and not observed) due to closely spaced band and $4f$ levels of the lanthanide [1].

Nevertheless, due to a number of properties such as excitation in the $4f$ - $5d$ transition region, large Stokes shift (about 1.6 eV), broad structureless band, decay in the microsecond time range, observed by us in LaF_3 - Sm^{2+} , luminescence resembles the anomalous luminescence of Eu^{2+} , Yb^{2+} MeF_2 crystals [1] and Eu^{2+} in LaF_3 [5].

It should also be noted that anomalous luminescence of Sm^{2+} in LaF_3 is observed simultaneously with $4f$ - $4f$ luminescence, which is unusual since both types of transitions should compete with each other. The intensity of the anomalous luminescence of LaF_3 - Sm^{2+} increases with heating in the temperature range 10–130 K, then decreases and disappears at 220–250 K. The growth of anomalous luminescence is accompanied by thermal quenching of f - f -luminescence, indicating competition in the population of their excited states. Apparently, thermally activated transfer from excited $4f(^5D_j)$ states of Sm^{2+} into the conduction

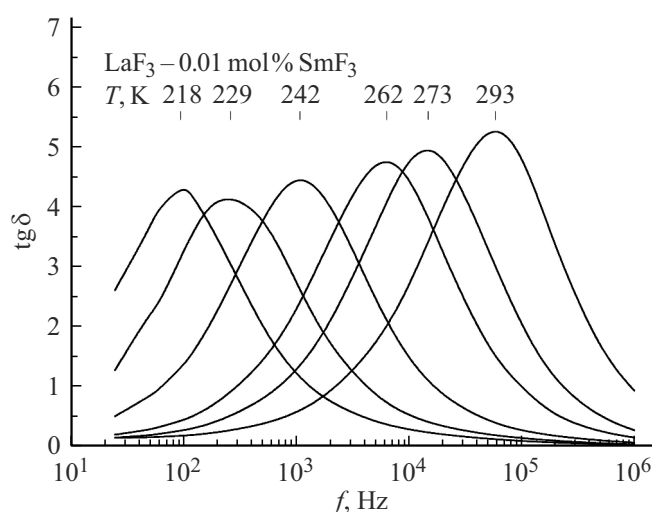


Figure 5. Frequency dependence curves of the loss tangent ($\text{tg } \delta$) of the LaF_3 -0.01 mol% SmF_3 crystal in the temperature range 218–293 K.

Comparison of absorption bands (λ_{abs}), luminescence bands (λ_{emis}), luminescence decay times (τ) and Stokes shifts (ΔS) of anomalous broadband luminescence in $\text{LaF}_3\text{-Eu}^{2+}$ crystals [5] and $\text{LaF}_3\text{-Sm}^{2+}$

Lanthanide	λ_{abs} , nm	λ_{emis} , nm/ τ , μs	ΔS , eV
Eu^{2+}	330	600/2.2	1.69
Sm^{2+}	460	1230/4.5	1.69

band causes the temperature increase in anomalous luminescence intensity.

Anomalous luminescence related to excitation in the $4f\text{-}5d$ transition wavelength region of Eu^{2+} and Sm^{2+} is found in LaF_3 crystals and is absent in CeF_3 .

The absolute Stokes shift for anomalous luminescence is the same in $\text{LaF}_3\text{-Eu}^{2+}$ and $\text{LaF}_3\text{-Sm}^{2+}$ (table).

Conclusion

The infrared luminescence band at 1230 nm in $\text{LaF}_3\text{-Sm}^{2+}$ crystals is due to anomalous luminescence, transitions from local relaxed band states of nearest lanthanide ions to the ground $4f$ state of samarium ions Sm^{2+} . No such luminescence band is detected in $\text{CeF}_3\text{-Sm}^{2+}$ crystals.

Anomalous luminescence is detected for the first time in the lanthanide Sm^{2+} for which both radiative $f\text{-}f$ -transitions and transitions from conduction band levels to the main $4f$ level of Sm^{2+} ions are observed simultaneously.

Acknowledgments

The author thanks V.A. Kozlovsky for growing the crystals studied in this work.

Funding

The research was carried out under the state assignment project No. 0284-2021-0004 (Materials and technologies for the development of radiation detectors, phosphors, and optical glasses). Part of the research was conducted at the Shared Equipment Center „Isotope-Geochemical Studies“ of the Vinogradov Institute of Geochemistry SB RAS.

Conflict of interest

The author declares that he has no conflict of interest.

References

- [1] P. Dorenbos. J. Physics: Condensed Matter, **15** (17), 2645 (2003). DOI: 10.1088/0953-8984/15/17/318
- [2] M. Grinberg, S. Mahlik. J. Non-crystalline Solids, **354** (35–39), 4163 (2008). DOI: 10.1016/j.jnoncrystol.2008.06.025
- [3] M. Hendriks, E. van der Kolk. J. Lumin., **207**, 231 (2019). DOI: 10.1016/j.jlumin.2018.11.018
- [4] B. Moine, B. Courtois, C. Pedrini. J. Physique, **50** (15), 2105 (1989). DOI: 10.1051/jphys:0198900500150210500
- [5] E.A. Radzhabov, R.Yu. Shendrik. Radiation Measurements, **90**, 80 (2016). DOI: 10.1016/j.radmeas.2016.02.012
- [6] C. van Aarle, K.W. Krämer, P. Dorenbos. J. Lumin., **266**, 120329 (2024). DOI: 10.1016/j.jlumin.2023.120329
- [7] C. van Aarle, K.W. Krämer, P. Dorenbos. J. Lumin., **251**, 119209 (2022). DOI: 10.1016/j.jlumin.2022.119209
- [8] R.H.P. Awater, M.S. Alekhin, D.A. Biner, K.W. Krämer, P. Dorenbos. J. Lumin., **212**, 1 (2019). DOI: 10.1016/j.jlumin.2019.04.002
- [9] J.J. Schuyt, J. Donaldson, G.V.M. Williams, S.V. Chong. J. Phys.: Condensed Matter, **32** (2), 025703 (2019). DOI: 10.1088/1361-648X/ab450d
- [10] M. Karbowski, P. Solarz, R. Lisiecki, W. Ryba-Romanowski. J. Lumin., **195**, 159 (2018). DOI: 10.1016/j.jlumin.2017.11.012
- [11] M.S. Alekhin, R.H. Awater, D.A. Biner, K.W. Krämer, J.T. de Haas, P. Dorenbos. J. Lumin., **167**, 347 (2015). DOI: 10.1016/j.jlumin.2015.07.002
- [12] E.A. Radzhabov, A.V. Samborsky. Bulletin of the Russian Academy of Sciences: Physics, **81** (9), 1058 (2017). DOI: 10.3103/S1062873817090209.
- [13] E.A. Radzhabov. Opt. Materials, **85**, 127 (2018). DOI: 10.1016/j.optmat.2018.08.044
- [14] D. Sofich, V. Gavrilenko, V. Pankratova, V. Pankratov, E. Kaneva, R. Shendrik. Crystals, **15** (6), 489 (2025). DOI: 10.3390/cryst15060489
- [15] L.C. Dixie, A. Edgar, C.M. Bartle. Nucl. Instrum. Methods Phys. Res. Sect. A Accel. Spectrom. Detect. Assoc. Equip., **753**, 131 (2014). DOI: 10.1016/j.nima.2014.03.038
- [16] G. Okada, Y. Fujimoto, H. Tanaka, S. Kasap, T. Yanagida. J. Rare Earths, **34** (8), 769 (2016). DOI: 10.1016/S1002-0721(16)60092-3
- [17] A. Roos, M. Buijs, K.E.D. Wapenaar, J. Schoonman. J. Phys. Chem. Solids, **46** (6), 655 (1985). DOI: 10.1016/0022-3697(85)90153-2
- [18] N.V. Popov, A.S. Mysovsky, N.G. Chuklina, E.A. Radzhabov. Bulletin of the Russian Academy of Sciences: Physics, **81** (9), 1141 (2017). DOI: 10.3103/S1062873817090192.
- [19] A.V. Samborsky, E.A. Radzhabov. AIP Conf. Proceedings, **2392** (1), 020007 (2021). DOI: 10.1063/5.0062750
- [20] E.A. Radzhabov, V.A. Kozlovskiy. Bulletin of the Russian Academy of Sciences: Physics, **79** (2) (2015). DOI: 10.3103/S1062873815020215.
- [21] P. Dorenbos. J. Lumin., **135**, 93 (2013). DOI: 10.1016/j.jlumin.2012.09.034

Translated by J.Savelyeva